Journal of Medicinal Chemistry

Article

pubs.acs.org/jmc

NHC Gold Halide Complexes Derived from 4,5-Diarylimidazoles: Synthesis, Structural Analysis, and Pharmacological Investigations as Potential Antitumor Agents

Wukun Liu,[†] Kerstin Bensdorf,[†] Maria Proetto,[†] Ulrich Abram,[‡] Adelheid Hagenbach,[‡] and Ronald Gust*[,†,§]

[†]Institute of Pharmacy, Freie Universität Berlin, Königin-Luise-Strasse, 2+4, 14195 Berlin, Germany

[‡]Institute of Chemistry and Biochemistry, Freie Universität Berlin, Fabeckstrasse 34-36, 14195 Berlin, Germany

[§]Institute of Pharmacy, University of Innsbruck, Innrain 52, A-6020 Innsbruck, Austria

Supporting Information

ABSTRACT: A series of novel neutral NHC gold halide complexes derived from 4,5-diarylimidazoles were synthesized, characterized, and analyzed for biological effects. High growth inhibitory effects in MCF-7 and MDA-MB 231 breast cancer as well as HT-29 colon cancer cell lines depended on the presence of the C4,C5-standing aromatic rings. Methoxy groups at these rings did not change the growth inhibitory properties, while F-substituents in the ortho-position (**5d**) increased the activity in MCF-7 and MDA-MB 231 cells. The substituents at the nitrogen atoms and the oxidation state of the metal play a subordinate role. The most active bromo[1,3-diethyl-4,5-bis(2-fluorophenyl)-1,3-dihydro-2*H*-imidazol-2-ylidene]gold(I) (**5d**) was distinctly more active than cisplatin. All complexes caused thioredoxin reductase (TrxR) inhibition (EC_{50} = 374−1505 nM) distinctly lower than auranofin (EC_{50} = 18.6 nM) excluding this enzyme as main target. Because of the low nuclear content, a participation of DNA interaction on the mode of action is very unlikely. The missing ER binding and the missing correlation of growth inhibition and inactivation of COX enzymes exclude these targets, too.

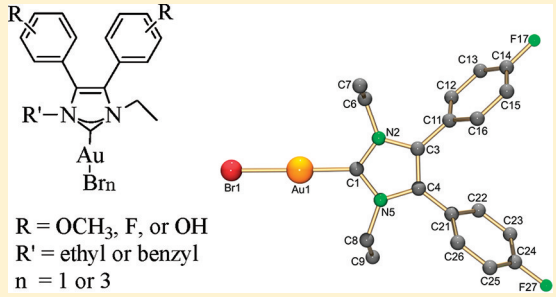

INTRODUCTION

Platinum-based drugs such as cisplatin or oxaliplatin are widely used in current tumor chemotherapy. However, severe side effects and frequent development of resistance phenomena complicate and hamper the clinical application.[1,2] A very promising strategy to overcome these obstacles is the use of specific carriers and the change from platinum to other transition metals.[1−4]

Among novel non-platinum based antitumor agents, gold complexes have recently gained attention because of their strong antiproliferative effects.[1,3−9] Two lead structures are auranofin, which is well-known for its antiarthritic properties, and its chloro analogue Et_3PAuCl (Scheme 1).

Scheme 1. Structures of Auranofin and Et_3PAuCl

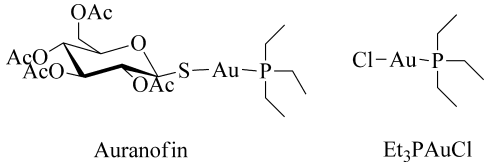

Auranofin Et_3PAuCl

Both complexes exhibit their antitumor activities due to inhibition of the enzyme thioredoxin reductase (TrxR).[1,3−11] In addition, previous structure−activity relationship (SAR) studies indicated that the phosphine ligand is more important for the biological potency than the halide or the thioglucose. Exchange of the carbohydrate ligand of auranofin (or the chlorine ligand of Et_3PAuCl) does not lead to a loss of antitumor activity.[4,11,12] Of late, there has been considerable interest in N-heterocyclic carbenes (NHCs) as alternatives to phosphines as ligands for the soft gold(I) ion. The relative ease of systematic modification of the NHC substituents and the comparable donor properties of NHCs to phosphines render NHCs attractive ligands.[3,4,8,13−26]

Recently, some NHC gold complexes were developed as antitumor agents. Cationic gold(I) carbenes are lipophilic compounds that are able to induce mitochondrial membrane permeabilization of rat liver mitochondria, as shown by Berners-Price et al.[1,3,4,6,8,14−20] Raubenheimer et al. reported a promising ferrocenylbis(carbene)gold(I) complex with an IC_{50} value in the range of those of cisplatin against Jurkat, CoLo 320 DM, and MCF-7 cells.[21] Also, antiproliferative activity has been described for a few simple neutral NHC gold(I) halide complexes[16,20,22−25] as well NHC gold(I) halides bound to biomolecules.[25] The structural modifications of these complexes mainly focus on variation of 1,3-N substituents at the imidazole core.

Received: August 30, 2011
Published: November 17, 2011

   dx.doi.org/10.1021/jm201156x | *J. Med. Chem.* 2011, 54, 8605−8615

Scheme 2. Synthesis Routes and Structures of Intermediates and NHC Gold Complexes[a]

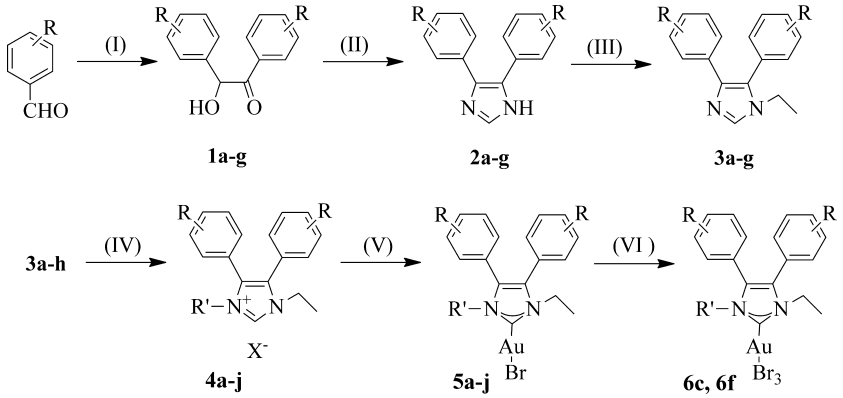

Compound	R	R'	X
1a, 2a, 3a, 4a, 5a	2-MeO	Et	Br
1b, 2b, 3b, 4b, 5b	3-MeO	Et	Br
1c, 2c, 3c, 4c, 5c, 6c	4-MeO	Et	Br
1d, 2d, 3d, 4d, 5d	2-F	Et	Br
1e, 2e, 3e, 4e, 5e	3-F	Et	Br
1f, 2f, 3f, 4f, 5f, 6f	4-F	Et	Br
1g, 2g, 3g, 4g, 5g	H	Et	Br
3h, 4h, 5h,	4-OH	Et	Br
4i, 5i	4-MeO	$PhCH_2$	Cl
4j, 5j	4-F	$PhCH_2$	Cl

[a]Reagents and conditions: (I) thiamine hydrochloride, water/ethanol 1:2, room temp, 2–7 days, 49–62%; (II) formamide, reflux, 3 h, 61–80%; (III) 95% NaH, ethyl bromide, absolute THF, reflux, 2 h, 68–88%; (IV) ethyl bromide or benzyl chloride, CH_3CN, reflux, 48–72 h, 72–84%. (V) Method A: LiHMDS, Me_2SAuCl, LiBr, DMF, room temp, 4 h, 45–84%. Method B: Ag_2O, CH_3OH/CH_2Cl_2 1:1.2, room temp, 12 h, then Me_2SAuCl, LiBr, room temp, 6 h, 28-48%. (VI) Br_2, CH_2Cl_2, room temp, 3 h, 83–85%.

In a previous study, we showed that NHC silver halide complexes possess good growth inhibitory effects against mammary and colon carcinoma cells.[27] Moreover, replacement of the phosphine in Et_3PAuCl by an NHC ligand with pharmacological activity (e.g., hormonal activity, cyclooxygenase inhibitory properties) could lead to new multitarget antitumor agents including the TxR.[3,5,9,23,25–29] Therefore, we focused our attention on the design of NHC gold complexes derived from pharmacologically active 4,5-diarylimidazoles.[28] To achieve a high accumulation grade in tumor cells, the aromatic rings were 2-OCH_3, 3-OCH_3, 4-OCH_3, 2-F, 3-F, 4-F, or 4-OH substituted. Such substitution patterns were already very successfully used in the case of [1,2-diarylethylenediamine]platinum(II) complexes.[29]

RESULTS AND DISCUSSION

Synthesis and Structural Characterization. The synthetic route to NHC gold derivatives is outlined in Schemes 2 and 3.

Precursors were synthesized according to our previously published methods.[27,28] Thus, **1a–g** were obtained from commercially available substituted benzaldehydes via the catalysis of thiamine hydrochloride. For ring closure, yielding the respective imidazoles **2a–g**, the benzoines **1a–g** were heated in formamide to reflux for 3 h. Reaction of **2a–g** with NaH and ethyl bromide in absolute THF afforded the corresponding

Scheme 3. Synthesis Route of 5k[a]

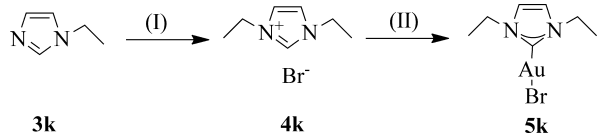

[a]Reagents and conditions: (I) ethyl bromide, CH_3CN, reflux, 48–72 h, 74.2%. (II) Method A: LiHMDS, Me_2SAuCl, LiBr, DMF, room temp, 4 h, 64.3%. Method B: Ag_2O, CH_3OH/CH_2Cl_2 1:1.2, room temp, 12 h, then Me_2SAuCl, LiBr, room temp, 6 h, 48%.

N-alkylations (**3a–g**).[27,28] The hydroxyl-substituted imidazole **3h** was generated from **3c** by ether cleavage with BBr_3.[28] Subsequent reaction of **3a–h** and commercially available **3k** with ethyl bromide in CH_3CN yielded the imidazolium salts **4a–g** and **4k**. The same reaction of **3c** and **3f** with benzyl chloride resulted in 1-benzyl-3-ethyl-4,5-diarylimidazolium chlorides **4i** and **4j**.

Two synthetic procedures were investigated for the synthesis of the NHC gold(I) complexes **5a–k**. The first procedure (method A) involves the treatment of a DMF solution of Me_2SAuCl with a solution containing an equimolar amount of **4a–k** (treated for deprotonation with lithium bis(trimethylsilyl)amide (LiHMDS)).

dx.doi.org/10.1021/jm201156x | J. Med. Chem. 2011, 54, 8605–8615

This procedure gave **5a**−**k** in high yields.[30] The second procedure (method B) involves the NHC−Ag(I) transfer method, whereby **4a**−**k** were treated with silver oxide in CH_2Cl_2, and the resulting NHC−Ag(I) complex was allowed to react with Me_2SAuCl.[30,31] This procedure gave **5a**−**k** in moderate yields. Further amounts of lithium bromide have to be present in both methods to ensure the exclusive formation of NHCAuBr (previous reports showed that the chloride in the complexes could be exchanged for bromide in the solution during the reaction[30,32]).

The oxidations of gold(I) complexes **5c** and **5f** were performed with bromine in dichloromethane at room temperature, resulting in the formation of an orange powder of the desired gold(III) complexes **6c** and **6f**.[25,33]

Precursors and the gold complexes were characterized by IR, NMR, and MS spectra. The IR spectra of ligands and complexes are very similar and not suitable to confirm the binding of NHC to gold. Analogously to NHC silver complexes,[27] the formation of the gold(I) complexes proceeded with the deprotonation of the (NCHN) proton of the imidazolium bromide salt. Consequently, the ^{1}H NMR spectrum of the respective gold complex lacks the characteristic NCHN resonance in the downfield region of the spectrum (Figure S1a in Supporting Information). The ^{13}C NMR spectrum, however, showed the appearance of the metal bound carbine (NCN−Au) peak at a much downfield shifted region ($\Delta\delta \approx 37$ ppm) which is comparable to those reported for other NHC gold(I) complexes (Figure S1b).[34] Furthermore, upon metal binding the ^{1}H NMR and ^{13}C NMR signals of ethyl, benzyl, and phenyl remain nearly unaffected (Figure S1).

The formation of complexes were further supported by positive mode ESI mass spectrometry, which documented a base peak corresponding to the $[M + Na]^+$ fragment for **5a**−**g**, **5i**−**k** and a base peak at m/z = 1089 corresponding to the $[2M - Br]^+$ fragment for **5h**.

The ^{1}H NMR spectra of the gold(III) complexes **6c** and **6f** were similar to the spectra of the corresponding gold(I) complexes **5c** and **5f**, while the NCN resonance in the ^{13}C NMR spectra of **6c** and **6f** are shifted upfield by 34.8 and 33.8 ppm compared to **5c** and **5f**, respectively (Figure S1). This strong upfield shift is surprising when compared to the downfield shift of the carbon atoms in the aromatic ring. As expected, this shift arises from the increased acidity of gold(III) due to an increase in the oxidation state.[25,33]

To gain insight into the coordination chemistry and structural parameters of these complexes, **5f** was isolated as single crystals by slow evaporation of a concentrated $MeOH/CH_2Cl_2$ solution and characterized by X-ray diffraction. The molecular structure of **5f** is depicted in Figure 1 and is a linear monocarbene gold(I) complex with common Au−$C_{carbene}$ and Au−Br bond lengths of 1.988(9) and 2.403(1) Å, respectively. The C(1)−Au(1)−Br(1) bond with an angle of 178.3(2)° is nearly linear.

An X-ray structure of **6f** could be obtained using the same method. **6f** has a four-coordinate gold atom in a square-planar environment, as expected for d^8 metals. The Br(3)−Au(1)−Br(4) and C(1)−Au(1)−Br(2) bonds are nearly linear, with angles of 175.93(5)° and 176.6(3)°. The C(1)−Au(1) distance is 2.005(8) Å, which is in accordance with published NHC gold(III) bromido complexes.[25,33] The Br−Au distances were found to be between 2.411(1) and 2.434(1) Å, with the Au−Br bond in trans position being slightly longer than other Au−Br bonds (Figure 2).

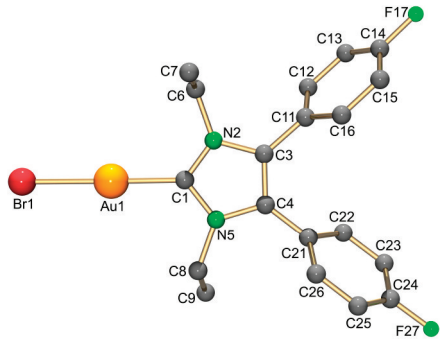

Figure 1. X-ray molecular structure of **5f**. Selected bond lengths (Å) and angles (deg) of **5f** are as follows: Au(1)−C(1) 1.988(9), Au(1)−Br(1) 2.403(1), C(1)−N(5) 1.32(1), C(1)−N(2) 1.362(12), C(1)−Au(1)−Br(1) 178.3(2), N(5)−C(1)−N(2) 105.8(7), N(5)−C(1)−Au(1) 126.8(7), N(2)−C(1)−Au(1) 127.4(6).

Table 1. Selected X-ray Data for 5f and 6f

parameter	5f	6f
crystal system	triclinic	orthorhombic
space group	$P\bar{1}$	*Pbca*
unit cell dimensions	a = 10.107(1) Å, α = 93.59(1)°	a = 11.536(1) Å
	b = 11.423(1) Å, β = 106.27(1)°	b = 15.954(1) Å
	c = 17.576(1) Å, γ = 90.33(1)°	c = 23.474(2) Å
volume	1943.5(3) Å^3	4320.3(6) Å^3
Z	4	8
density (calculated)	2.014 Mg/m^3	2.303 Mg/m^3
absorption coefficient	9.647 mm^{-1}	12.383 mm^{-1}
F(000)	1112	2784
crystal size	0.50 × 0.23 × 0.03 mm^3	0.34 × 0.15 × 0.10 mm^3
θ range for data collection	1.79−26.00°	1.74−29.27°
index range	$-12 \le h \le 12$, $-14 \le k \le 14$, $-20 \le l \le 21$	$-15 \le h \le 12$, $-21 \le k \le 21$, $-31 \le l \le 32$
reflections collected	14995	42667
independent reflections	7458 [R_{int} = 0.1039]	5847 [R_{int} = 0.1481]
absorption correction	numerical	integration
max and min transmission	0.4848 and 0.1871	0.3731 and 0.1138
data/restraints/parameters	7458/0/452	5847/0/244
goodness-of-fit on F^2	0.840	0.830
final R indices [$I > 2\sigma(I)$]	R1 = 0.0535, wR2 = 0.1304	R1 = 0.0550, wR2 = 0.1365
R indices (all data)	R1 = 0.0711, wR2 = 0.1417	R1 = 0.1034, wR2 = 0.1713
largest diff peak and hole	3.591 and −2.647 e·Å^{-3}	0.960 and −3.829 e·Å^{-3}

No aurophilic interactions have been observed in the solid state structure of both complexes, which is most likely due to the steric bulk of the carbene ligand.

Finally, all novel gold complexes are sufficiently stable in solid state and solution. If the complexes were dissolved in $CDCl_3$, methanol-d_4, methanol-d_4/D_2O (1:1), or DMSO-d_6, no changes of the spectra were observed during the storage at room temperature. Furthermore, HPLC analysis of aqueous solutions demonstrated sufficient stability and no degradation during 24 h.

dx.doi.org/10.1021/jm201156x | J. Med. Chem. 2011, 54, 8605−8615

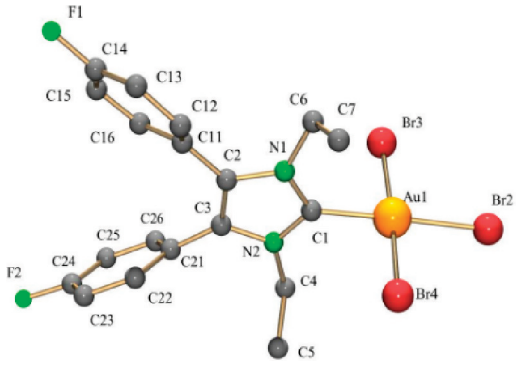

Figure 2. X-ray molecular structure of **6f**. Selected bond lengths (Å) and angles deg) of **6f** are as follows: Au(1)−C(1) 2.005(8), Au(1)−Br(2) 2.434(1), Au(1)−Br(3) 2.411(1), Au(1)−Br(4) 2.421(1), C(1)−Au(1)−Br(3) 87.5(3), C(1)−Au(1)−Br(4) 88.9(3), Br(3)−Au(1)−Br(4) 175.93(5), C(1)−Au(1)−Br(2) 176.6(3), Br(3)−Au(1)−Br(2) 91.45(4), Br(4)−Au(1)−Br(2) 92.24(4), N(1)−C(1)−Au(1) 127.7(7), N(2)−C(1)−Au(1) 124.5(7).

Antiproliferative Effects. In vitro cytotoxicity assays were performed to get an insight into the antitumor activity of the neutral gold complexes. All complexes and the established antitumor drug cisplatin were screened against MCF-7, MDA-MB 231 breast cancer cells, and HT-29 colon cancer cells. The experiments were performed according to established procedures.[10,11,35] IC_{50} values of the selected intermediate **4f**, the gold complexes **5a**−**k**, **6c**, **6f**, and cisplatin determined after 72 h of incubation are shown in Table 2. The time dependent antiproliferative effects of **5c** and **5f** at the three cancer cell lines are presented in Figure 3.

Table 2. Growth-Inhibitory Effects against Breast Cancer and Colon Cancer Cells[a]

	cytotoxicity (IC_{50}, μM)		
compd	MCF-7	MDA-MB 231	HT-29
4f	>50	>50	>50
5a	1.2 ± 0.1	2.4 ± 0.5	3.1 ± 0.4
5b	1.6 ± 0.6	2.9 ± 0.3	4.2 ± 1.0
5c	1.4 ± 0.1	3.7 ± 0.9	2.9 ± 0.1
5d	0.80 ± 0.06	1.7 ± 0.9	3.3 ± 1.0
5e	3.1 ± 0.1	6.4 ± 0.1	4.2 ± 0.3
5f	1.1 ± 0.3	3.9 ± 0.1	2.3 ± 0.1
5g	0.87 ± 0.07	3.1 ± 0.5	3.3 ± 0.7
5h	4.5 ± 0.3	>20	17.0 ± 2.8
5i	2.6 ± 0.3	3.3 ± 0.7	4.3 ± 0.1
5j	1.8 ± 0.1	2.4 ± 0.1	3.2 ± 0.3
5k	3.0 ± 0.4	6.9 ± 0.8	7.7 ± 0.8
6c	1.9 ± 0.1	4.4 ± 1.1	6.2 ± 1.0
6f	1.9 ± 0.4	4.4 ± 0.7	7.5 ± 2.9
auranofin[b]	1.1	*d*	2.6
Et_3AuCl[c]	3.2	*d*	5.3
cisplatin	1.6 ± 0.5	7.8 ± 0.8	4.1 ± 0.3

[a]The IC_{50} value was determined as the concentration causing 50% decrease in cell growth after 72 h of incubation and calculated as the mean of at least two or three independent experiments. [b]Data from ref 11. [c]Data from refs 10 and 11. [d]Not measured.

Cisplatin characteristically reduced the cell growth of MCF-7 (IC_{50} = 1.6 μM), MDA-MB 231 (IC_{50} = 7.8 μM), and HT-29 (IC_{50} = 4.1 μM) cells. According to our previous reports, auranofin caused effects comparable to those of cisplatin against MCF-7 cells (IC_{50} = 1.1 μM) and was slightly more active against HT-29 cells (IC_{50} = 2.6 μM).[11] Et_3PAuCl was less active at MCF-7 and HT-29 cell lines (IC_{50} of 3.2 and 5.3 μM, respectively).[10,11]

Exchange of the triethylphophine ligand by 1,3-diethyl-1,3-dihydro-2*H*-imidazol-2-ylidene in Et_3PAuCl as well as the exchange of the chloride by bromide did not change the activity against MCF-7 cells (**5k**, IC_{50} = 3.0 μM) but reduced the effects against HT-29 cells (**5k**, IC_{50} = 7.7 μM). At the MDA-MB 231 cell line **5k** caused an IC_{50} = 6.9 μM, similar to cisplatin. Introduction of phenyl rings at C4 and C5 of the heterocycle (**5k** → **5g**) increased the growth inhibitory effects (IC_{50} = 0.87 μM at MCF-7 cells, IC_{50} = 3.1 μM at MDA-MB 231 cells, IC_{50} = 3.3 μM at HT-29 cells). **5g** was even more active than cisplatin.

As outlined in Table 2, methoxy substituents at the aromatic rings (**5g** → **5a**,**b**,**c**) did not change the growth inhibitory properties of **5g**, while F substituents in the ortho-position (**5d**) increased the activity against MDA-MB 231 cells (IC_{50} = 1.7 μM) and reduced the activity at all cell lines in meta-position (**5e**, IC_{50} = 3.1 μM at MCF-7 cells, IC_{50} = 6.4 μM at MDA-MB 231 cells, IC_{50} = 4.2 μM at HT-29 cells). The results of **5f** bearing a 4-F substituent are comparable to those of **5g** (unsubstituted) and **5c** (4-OCH_3).

Exchange of the 4-OCH_3 groups by more hydrophilic 4-OH groups (**5c** → **5h**) strongly decreased the cytotoxicity (**5h**, IC_{50} = 4.5 μM at MCF-7 cells, IC_{50} > 20 μM at MDA-MB 231 cells, IC_{50} = 17.0 μM at HT-29 cells). This substitution effect was already observed during the study of other metal complexes such as [1,2-diarylethylenediamine]platinum(II)[29] or [diarylsalene]-iron complexes.[36]

The substituents at the nitrogen atoms seem to play a subordinate role because complexes with either an N1-ethyl chain or a bulky N1-benzyl moiety yielded nearly identical results (compare **5c** and **5i** as well as **5f** and **5j**, Table 2).

Finally the growth inhibitory effects depended on the presence of a metal center (the imidazoles were inactive; e.g., see **4f** in Table 2). Interestingly, the relevance of the oxidation state for the growth inhibition of MCF-7 and MDA-MB 231 cells was low. At the HT-29 cell line only, the Au(III) complexes **6c** and **6f** were less active than their Au(I) congeners **5c** and **5f**. Moreover, these novel gold complexes were distinctly more active than the corresponding silver complexes[27] and benzimidazol-2-ylidene gold complexes[23] tested in the same assay.

Time-dependent cytotoxicity studies were performed on the examples of **5c** and **5f**. The curves presented in Figure 3 indicate for **5f** a recuperation of HT-29 cells at concentrations below 2.5 μM and of MCF-7 cells below 1 μM. Because exponential cell growth is guaranteed for at least 140 h of incubation, the rise of the growth curve can be explained by the development of drug resistance.[35,36]

In contrast to cisplatin (Figure S2), which reached its maximum effect toward the end of the test, the onset of antiproliferative effects of **5c** and **5f** was observed much earlier. Both complexes showed their maximum of activity after 48 h. In the case of **5c**, the growth inhibition holds during the whole time of incubation (no recuperation of the tumor cells after a prolonged time of exposition).

Inhibition of the Enzyme TrxR. As discussed above (Introduction), the TrxR must be considered as target because it is involved in various tumor related biochemical pathways and inactivation causes reduced tumor cell growth.[3−6,9,23,24,26,37−40] Auranofin and related gold complexes demonstrated strong

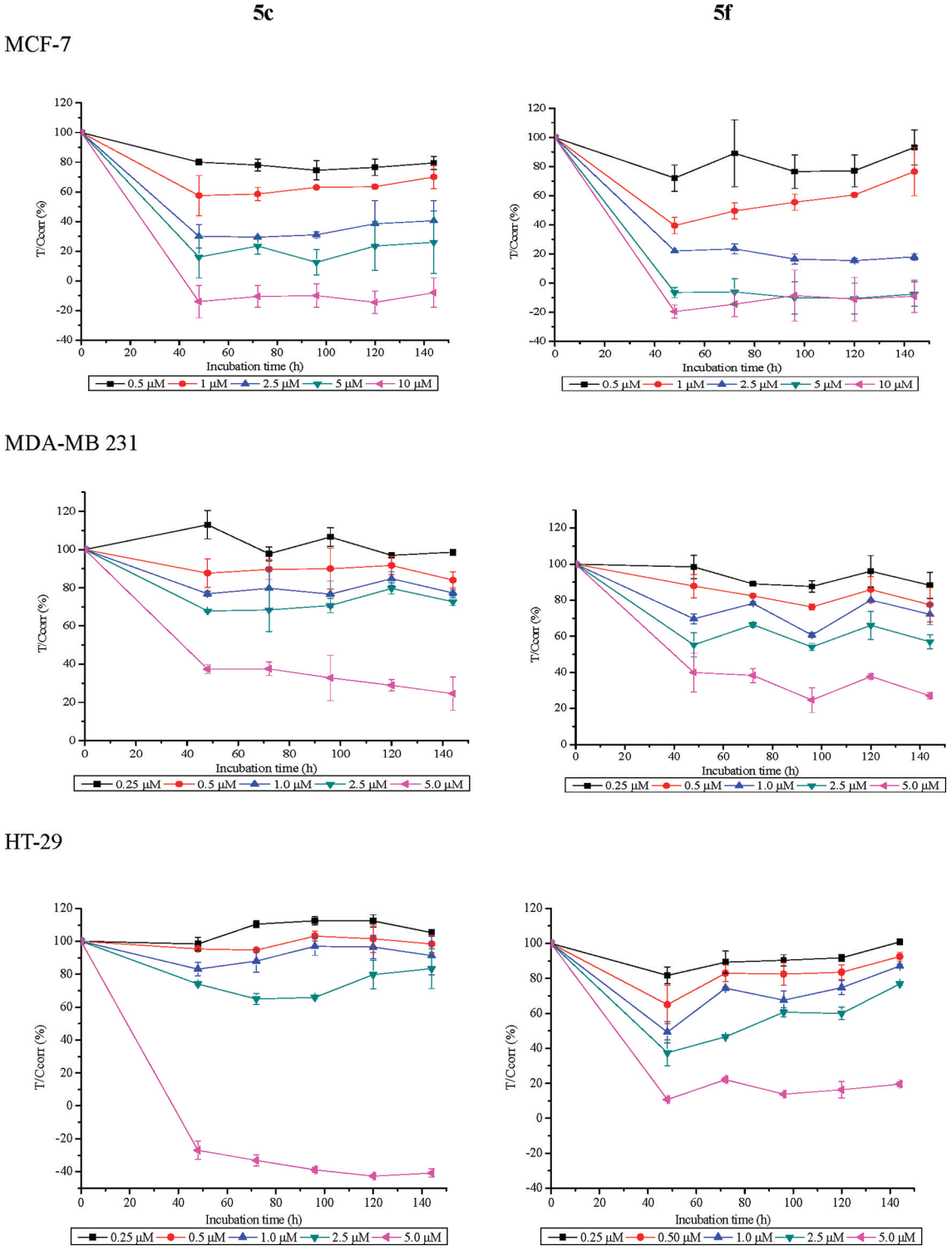

Figure 3. Time-dependent antiproliferative effects of complexes **5c** (left) and **5f** (right) on MCF-7, MDA-MB 231, and HT-29 cells.

affinity for TrxR leading to inactivation due to the formation of a covalent bond at the Se center of the enzyme.[3−6,9,23,24,26,37−39]

The inhibitory potentials of all gold complexes, **4f** (as example of the free ligands) as well as Et_3PAuCl and auranofin (as positive controls), were studied by the dithiobisnitrobenzoic acid (DTNB) reduction assay using isolated rat liver TrxR. This assay makes use of the fact that TrxR reduces the disulfide bonds of DTNB with formation of 2-nitro-5-thionitrobenzoic acid (TNB), which can be detected photometrically.

With the exception of the complex **5h**, which showed low solubility in the used assay buffer that might explain its significantly lower activity, all gold complexes displayed activity against TrxR (IC_{50} of 0.374−1.505 μM). They are comparably active as benzimidazol-2-ylidene gold complexes[23] but less active than Et_3PAuCl and auranofin (IC_{50} of 25.8 and 18.6 nM, respectively). As expected, the inhibitory effect depends on the presence of a gold center; **4f** was completely inactive (IC_{50} > 50 μM). A clear structure−activity relationship is not given by the data

dx.doi.org/10.1021/jm201156x | J. Med. Chem. 2011, 54, 8605−8615

listed in Table 3, and a correlation with the growth inhibition is missing. Therefore, besides the TrxR interaction, further targets must be considered as part of the mode of action.[3,4,9,40−46]

Table 3. Inhibition of TrxR

compd	TrxR[a] (IC_{50}, nM)	compd	TrxR[a] (IC_{50}, nM)
4f	>50000	**5h**	4371.3 ± 322.2
5a	597.5 ± 89.6	**5i**	802.7 ± 68.1
5b	668.3 ± 38.1	**5j**	374.4 ± 9.0
5c	1505.5 ± 27.3	**5k**	379.8 ± 105.1
5d	703.9 ± 61.5	**6c**	621.6 ± 51.3
5e	1202.0 ± 110.3	**6f**	903.6 ± 1.1
5f	815.4 ± 74.1	auranofin	18.6 ± 7.2
5g	1036.1 ± 40.4	Et_3PAuCl	25.8 ± 13.0

[a]The IC_{50} values were calculated as the concentration of compound decreasing the enzymatic activity of the untreated control by 50% and are given as the mean and error of three experiments.

Reaction with Glutathione. It is a well-known fact that cisplatin and other metal containing drugs including auranofin are very reactive toward thiols such as the tripeptide glutathione.[1,3−5,23] The levels of glutathione in tumor cells reach the low millimolar range and are made responsible for inactivation and drug resistance phenomena. Therefore, it was of interest to study the interaction with glutathione under physiological conditions.

In the used assay, an excess of the respective gold complexes (166.7 μM) with reduced glutathione was incubated at 37 °C for 20 and 60 min. Oxidized GSH reduces analogously to TrxR DTNB to TNB. Me_2SAuCl (33% 20 min; 56% 60 min) used as positive control led to reduced TNB formation under the chosen conditions (Figure 4), while auranofin (194% 20 min; 212% 60 min) strongly increased the TNB release during the reaction.[23] A DMSO control was set as 100%.

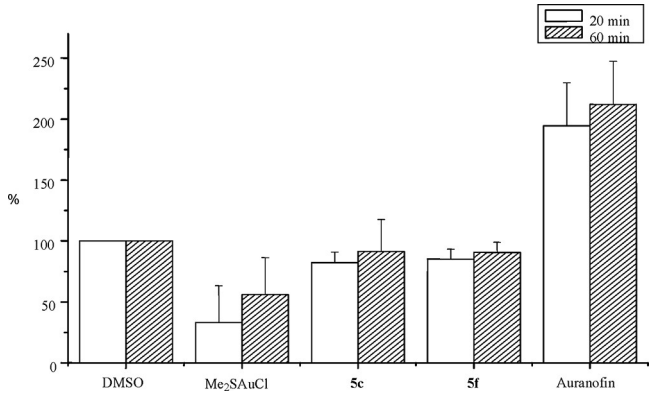

Figure 4. Interaction of gold complexes (166.7 μM) with glutathione and DTNB. Percentage building of TNB after 20 and 60 min of incubation.

Interestingly, the complexes determined in the examples of **5c** (82%, 20 min; 91%, 60 min) and **5f** (85%, 20 min; 90%, 60 min) did not significantly influence the reaction and can thus be considered as sufficiently stable against thiols under biologically relevant conditions, a property highly desirable in the drug development of novel metal coordination compounds.[23]

Cellular and Nuclear Uptake as Well as DNA Interaction. Because the cytotoxic effects of metal complexes in cell culture experiments were strongly influenced by cellular uptake and accumulation, the intracellular drug level in MCF-7 and HT-29 cells was studied in the examples of **5c**, **5f**, and Et_3PAuCl.

In the present study we used a recently described electrothermal atomic absorption spectroscopy (ETAAS) method, which was developed for the bioanalysis of gold complexes and based on the standard addition method.[10,47] Experiments were performed using an extracellular concentration of 10 μM and a short exposure period of 6 h to avoid a loss of cell biomass due to toxic effects. Results were corrected for the respective protein contents of the samples, and values are accordingly presented as ng of metal/mg of protein.

MCF-7 cells incubated with either **5c** or **5f** showed about a 3-fold higher gold content (**5c**, 134.2 ng/mg; **5f**, 67.2 ng/mg) than HT-29 cells (**5c**, 41.4 ng/mg; **5f**, 21.9 ng/mg). However, the individual cellular parameters must be taken into account. From the mean cellular diameter and the mean protein to volume ratio of HT-29[47] and MCF-7 cells,[48] it can be estimated that 1.0 ng of Au per mg of protein corresponds to a cellular molar concentration of 1.0 μM in HT-29 cells but to only 0.57 μM in MCF-7 cells. Nevertheless, the cellular molar concentrations of **5c** and **5f** were higher in MCF-7 cells (76.5 and 38.3 μM, respectively) than in HT-29 cells (41.4 and 21.9 μM, respectively).

The uptake in HT-29 cells corresponded with that of the references cisplatin and Et_3PAuCl, while it strongly differed in MCF-7 cell: **5f** ∼ cisplatin < **5c** < Et_3PAuCl. The highest intracellular metal content of 52.4 ng/mg was achieved with Et_3PAuCl.

To get information on whether the complexes might reach the major target of metal complexes, the DNA, the nuclei of MCF-7 and HT-29 cells treated with **5c**, **5f**, or Et_3PAuCl were isolated by a short sucrose gradient and investigated for their gold content using ETAAS. The results were calculated as ng of Au/mg of nuclear protein (Table 4).

Similar to the cellular uptake, the nuclear gold content was higher in MCF-7 than in HT-29 cells. Interestingly, **5c** and Et_3PAuCl caused nearly the same values (212.1 and 176.8 ng/mg, respectively) which are 2-fold higher than that of **5f** (81.4 ng/mg). In the nuclei of HT-29 cells only small amounts of gold (14.8 ng/mg (**5c**), 9.5 ng/mg (**5f**), and 56.6 ng/mg (Et_3PAuCl)) were detected. These findings did not correlate with the growth inhibitory potency. Therefore, we generally investigated the DNA binding properties using salmon testes DNA (Table 4). In this test **5c** and **5f** showed a moderate binding to DNA (**5c**, 2.03 pmol/μg; **5f**, 1.03 pmol/μg) after 4 h, not as high as cisplatin (14.2 pmol/μg) but higher than Et_3PAuCl (0.11 pmol/μg).

On the basis of these results, it is not very likely that DNA interaction causes the cytotoxic effects of the gold complexes.

ER Interaction and the Inhibition of COX. The missing correlation between cellular uptake, DNA binding, TrxR-inhibition, and cytotoxicity induced us to search for further targets of the novel gold complexes.

As the NHC ligands described in this paper are derivatives of 2,4,5-triarylimidazoles designed as estrogen receptor (ER) ligands,[28,49−51] we investigated if the ER is involved in the mode of action in MCF-7 cells. For this purpose, ERα-positive MCF-7 breast cancer cells, stably transfected with the plasmid ERE_{wtc}luc (MCF-7-2a cells) and U2-OS cells transiently transfected with the plasmid pSG5-ERα (U2-OS/α) or pSG5-ERβ FL (U2-OS/β) and the reporter plasmid p(ERE)2-luc+ were used to evaluate ER subtype selectivity on the molecular level.[28,49−51] Unfortunately, all complexes did not induce agonistic or antagonistic

dx.doi.org/10.1021/jm201156x | J. Med. Chem. 2011, 54, 8605−8615

Table 4. Cellular, Nuclear Uptake, and DNA Binding Efficiency of the Complexes

	cellular uptake[a]						
	ng of metal/mg of protein		μM		nuclear uptake[a] (ng of Au/mg of nuclear protein)		
compd	MCF-7	HT-29	MCF-7	HT-29	MCF-7	HT-29	DNA binding[b] (pmol/μg)
5c	134.2 ± 29.1	41.4 ± 9.9	76.5	41.4	212.1 ± 14.2	14.8 ± 0.8	2.03 ± 0.08
5f	67.2 ± 9.3	21.9 ± 2.1	38.3	21.9	81.4 ± 36.5	9.5 ± 4.1	1.03 ± 0.11
Et_3PAuCl	282.1 ± 22.8	52.4 ± 1.6	160.8	52.4	176.8 ± 80.3	56.6 ± 14.3	0.11 ± 0.02
cisplatin	40.9 ± 5.7	28.6 ± 3.6	23.3	28.6	*c*	*c*	14.2 ± 1.4

[a]Results were calculated from the data of three independent experiments. [b]Results were calculated as the mean of at least two independent experiments, which were performed with two replicates. [c]Not measured.

properties (data not shown). Therefore, an ER-mediated cytotoxicity can be excluded.

A further possible target of triarylimidazole derivatives are the cyclooxygenase enzymes (COX-1/2), as we demonstrated in an earlier study.[51] Both subtypes are the targets not only for the design of anti-inflammatory drugs but also in cancer chemotherapy.[51] For Co-ASS, a metallodrug of aspirin, a mode of action involving COX inhibition was postulated. The complex possessed high cytotoxicity and represented by far a more efficient COX inhibitor than aspirin.[52−54] Recently, it was demonstrated that auranofin inhibited the formation of eicosanoids related to the activity of COX-1 and 12-lipoxygenase (LOX) in human platelets.[4]

On the basis of these facts, the relative COX inhibition was determined exemplarily for complex **5f** and its ligand **4f**. The effects of the compounds on isolated COX-1 and COX-2 enzymes were quantified by ELISA in a concentration of 10 μM. Aspirin was used for comparison. At the concentration used aspirin showed only marginal activity at COX-1 (29% inhibition) and was inactive at COX-2. Interestingly, in contrast to its ligand **4f** which was inactive at both isoenzymes, **5f** selectively inhibited COX-1 (100%). Participation on the growth inhibitory effects against MCF-7 might be possible, since these cells have a basal level of COX-1 and a barely detectable and transient COX-2 inducible expression, whereas MDA-MB 231 cells show a low expression of COX-1 but a constitutive level of COX-2.[55] Therefore, their growth is sensitive to NSAID treatment[56,57] The data listed in Table 2 indicate for **5f** a comparable activity against both cell lines. Therefore, COX-inhibition is also very unlikely as the mode of action.

Nevertheless it is worthy to note that **5f** is an effective COX-1 inhibitor, which makes this class of complexes an interesting subject for further SAR study.

CONCLUSION

4,5-Diarylimidazole derivatives were synthesized as NHC ligands for gold complexes. The inactive ligands modulate the biological activity of the complexes. NHC gold halides caused growth inhibitory effects dependent on the substituents at the aromatic rings against MCF-7 and MDA-MB 231 breast as well as HT-29 colon cancer cell lines. The influence of N-substituents and the oxidation state of the metal (Au(I) or Au(III)) is relatively low. All complexes inhibited the TrxR. The missing SAR and the missing correlation with cytotoxic properties indicated the involvement of further targets. On the basis of the investigations of cellular and nuclear uptake, as well as the binding to the ER, DNA binding and interference in the hormonal system can be excluded. The selective inhibition of the COX-1 enzyme by complex **5f** opens a new perspective for use of NHC gold complexes in medicinal chemistry.

EXPERIMENTAL SECTION

General. The following instrumentation was used: IR spectra (KBr pellets), Perkin-Elmer model 580 A (Shelton, U.S.); ^1H or ^{13}C NMR spectra, Bruker ADX 400 spectrometer operated at 400 or 100 MHz (internal standard, tetramethylsilane); electron impact (EI) MS spectra, Varian CH-7A (70 eV) spectrometer; ESI-TOF spectra, Agilent 6210 ESI-TOF, Agilent Technologies, Santa Clara, CA, U.S.; elemental C, H, N analysis, PerkinElmer 240 B and C analyzer. All complexes reported in the manuscript have a purity of >95%. Chemicals were obtained from Sigma-Aldrich (Germany) and used without further purification. Reactions were all monitored by TLC, performed on silica gel plates 60 F254 (Merck, Darmstadt/Germany). Visualization on TLC was achieved by UV light. Column chromatography was performed with Merck silica gel 60H, grain size of <0.063 mm, 230 mesh ASTM (Darmstadt/Germany).

General Procedure for the Synthesis of 5a−k. Method A. LiHMDS (104 mg, 0.62 mmol) was added to a solution of the imidazolium salt (0.55 mmol) in DMF (5 mL). After the resulting mixture was stirred for 15 min a solution of Me_2SAuCl (162 mg, 0.55 mmol) and LiBr (477 mg, 5.5 mmol) in DMF (1 mL) was added and the suspension stirred for additional 4 h. Then water (10 mL) was added and a gray precipitate formed. The precipitate was collected and washed with water (3 × 10 mL). Column chromatography on silica gel (CH_2Cl_2/petroleum ether) followed by recrystallization from CH_2Cl_2/*n*-hexane yielded pure gold complexes.

Method B. An amount of 0.16 mmol of imidazolium salt in a mixture of CH_2Cl_2 (1 mL) and methanol (1.2 mL) was combined with solid silver(I) oxide (21 mg, 0.09 mmol) under N_2 atmosphere and stirred overnight under protection from light. Then Me_2SAuCl (47 mg, 0.16 mmol) and LiBr (139 mg 1.6 mmol) were added and the suspension was stirred for an additional 6 h under N_2. The gray precipitate was separated by filtration over a bed of Celite and the filtrate was evaporated to dryness under reduced pressure to yield a colorless oil. Column chromatography on silica gel (CH_2Cl_2/petroleum ether) followed by recrystallization from CH_2Cl_2/*n*-hexane yielded pure gold complexes.

Bromo[1,3-diethyl-4,5-bis(2-methoxyphenyl)-1,3-dihydro-2*H*-imidazol-2-ylidene]gold(I) 5a. Method A: yield 56.7% of a white solid. ESI-MS *m*/*z*: 337 $[M - AuBr]^+$, 635 $[M + Na]^+$, 869 $[2M - AuBr_2]^+$, 1145 $[2M - Br]^+$. IR (KBr, cm^{-1}): 3061, 2955, 2921, 2851, 1632, 1603, 1461, 1248, 1179, 1023, 756. ^1H NMR ($CDCl_3$): δ 1.27 (t, 6H, CH_2CH_3, J = 7.2 Hz), 3.81 (s, 6H, OCH_3), 4.10 (q, 4H, CH_2CH_3, J = 7.2 Hz), 6.81−6.97 (m, 5H, ArH), 7.10−7.12 (m, 1H, ArH), 7.30−7.34 (m, 2H, ArH). Anal. ($C_{21}H_{24}AuBrN_2O_2$) C, H, N.

Bromo[1,3-diethyl-4,5-bis(3-methoxyphenyl)imidazol-2-ylidene]gold(I) 5b. Method A: yield 78.9% of a pale yellow solid. ESI-MS *m*/*z*: 635 $[M + Na]^+$, 869 $[2M - AuBr_2]^+$, 1145 $[2M - Br]^+$, 1861 $[3M + Na]^+$, 1877 $[3M + K]^+$. IR (KBr, cm^{-1}): 3065, 2955, 2920, 2850, 1630, 1601, 1460, 1238, 1176, 1040, 701. ^1H NMR ($CDCl_3$): δ 1.33 (t, 6H, CH_2CH_3, J = 7.2 Hz), 3.73 (s, 6H, OCH_3), 4.20 (q, 4H, CH_2CH_3, J = 7.2 Hz), 6.71−6.80 (m, 4H, ArH), 6.89−6.91 (m, 2H, ArH), 7.26−7.29 (m, 2H, ArH). ^{13}C NMR ($CDCl_3$): δ 17.0 (s, CH_3); 44.3 (s, CH_2); 55.3 (s, OCH_3); 114.7, 116.2, 122.7, 128.9, 129.9, 130.8, 159.6 (s, C_{Ar}); 172.7 (s, NCN). Anal. ($C_{21}H_{24}AuBrN_2O_2$) C, H, N.

dx.doi.org/10.1021/jm201156x | J. Med. Chem. 2011, 54, 8605−8615

Bromo[1,3-diethyl-4,5-bis(4-methoxyphenyl)imidazol-2-ylidene]gold(I) 5c. Method A: yield 73.4%. Method B: yield 45.1% of a white solid. ESI-MS m/z: 635 $[M + Na]^+$, 869 $[2M - AuBr_2]^+$, 1145 $[2M - Br]^+$. IR (KBr, cm^{-1}): 3065, 2967, 2930, 2841, 1630, 1505, 1251, 1178, 1026, 843. ^1H NMR ($CDCl_3$): δ 1.30 (t, 6H, CH_2CH_3, J = 7.2 Hz), 3.80 (s, 6H, OCH_3), 4.16 (q, 4H, CH_2CH_3, J = 7.2 Hz), 6.86 (d, 4H, ArH, J = 8.4 Hz), 7.10 (d, 4H, ArH, J = 8.8 Hz). ^{13}C NMR ($CDCl_3$): δ 16.9 (s, CH_3); 44.1 (s, CH_2); 55.2 (s, OCH_3); 114.3, 119.8, 130.6, 131.7, 160.1 (s, C_{Ar}); 172.1 (s, NCN). Anal. ($C_{21}H_{24}AuBrN_2O_2$) C, H, N.

Bromo[1,3-diethyl-4,5-bis(2-fluorophenyl)imidazol-2-ylidene]gold(I) 5d. Method A: yield 79.9% of a white solid. ESI-MS m/z: 611 $[M + Na]^+$, 627 $[M + K]^+$, 821 $[2M - AuBr_2]^+$, 859 $[2M - AuBr_2+K]^+$, 1097 $[2M - Br]^+$, 1217 $[2M + K]^+$. IR (KBr, cm^{-1}): 3061, 2955, 2921, 2851, 1632, 1484, 1456, 1229, 1107, 762. ^1H NMR ($CDCl_3$): δ 1.31 (t, 6H, CH_2CH_3, J = 7.2 Hz), 4.14 (q, 4H, CH_2CH_3, J = 7.2 Hz), 7.10–7.19 (m, 6H, ArH), 7.38–7.44 (m, 2H, ArH). ^{13}C NMR ($CDCl_3$): δ 16.6 (s, CH_3); 44.7 (s, CH_2); 115.1, 115.2, 116.1, 116.3, 124.7, 126.4 (s, C_{Ar}); 132.3 (d, C_{Ar}); 132.5, 159.2, 161.7 (s, C_{Ar}); 174.0 (s, NCN). Anal. ($C_{19}H_{18}AuBrF_2N_2$) C, H, N.

Bromo[1,3-diethyl-4,5-bis(3-fluorophenyl)imidazol-2-ylidene]gold(I) 5e. Method A: yield 84.5% of a white solid. ESI-MS m/z: 611 $[M + Na]^+$, 627 $[M + K]^+$, 821 $[2M - AuBr_2]^+$, 1097 $[2M - Br]^+$, 1217 $[2M + K]^+$. IR (KBr, cm^{-1}): 3055, 2954, 2919, 2851, 1608, 1580, 1462, 1187, 791. ^1H NMR ($CDCl_3$): δ 1.35 (t, 6H, CH_2CH_3, J = 7.2 Hz), 4.23 (q, 4H, CH_2CH_3, J = 7.2 Hz), 6.92–7.02 (m, 4H, ArH), 7.11–7.16 (m, 2H, ArH), 7.33–7.42 (m, 2H, ArH). ^{13}C NMR ($CDCl_3$): δ 16.9 (s, CH_3); 44.5 (s, CH_2); 116.7, 117.0, 117.4, 117.6 (s, C_{Ar}); 126.3 (d, C_{Ar}); 129.3, 129.4 (s, C_{Ar}); 130.1 (d, C_{Ar}); 130.7, 130.8, 161.4, 164.1 (s, C_{Ar}); 173.8 (s, NCN). Anal. ($C_{19}H_{18}AuBrF_2N_2 \cdot 0.1$ n-hexane) C, H, N.

Bromo[1,3-diethyl-4,5-bis(4-fluorophenyl)imidazol-2-ylidene]gold(I) 5f. Method A: yield 78.2%. Method B: yield 48.7% of a white solid. ESI-MS m/z: 611 $[M + Na]^+$, 821 $[2M - AuBr_2]^+$. IR (KBr, cm^{-1}): 3061, 2966, 2924, 2851, 1631, 1601, 1503, 1460, 1228, 1159, 1094, 843. ^1H NMR ($CDCl_3$): δ 1.31 (t, 6H, CH_2CH_3, J = 7.2 Hz), 4.18 (q, 4H, CH_2CH_3, J = 7.2 Hz), 7.07 (t, 4H, ArH, J = 8.4 Hz), 7.16–7.20 (m, 4H, ArH). ^{13}C NMR ($CDCl_3$): δ 16.9 (s, CH_3); 44.3 (s, CH_2); 116.2, 116.4 (s, C_{Ar}); 123.4 (d, C_{Ar}); 130.3, 132.3, 132.4, 161.9, 164.4 (s, C_{Ar}); 173.2 (s, NCN). Anal. ($C_{19}H_{18}AuBrF_2N_2$) C, H, N.

Bromo[1,3-diethyl-4,5-diphenylimidazol-2-ylidene]gold(I) 5g. Method A: yield 82.2% of a white solid. ESI-MS m/z: 575 $[M + Na]^+$, 591 $[M + K]^+$, 749 $[2M - AuBr_2]^+$, 1025 $[2M - Br]^+$. IR (KBr, cm^{-1}): 3056, 2955, 2923, 2852, 1629, 1487, 1461, 1375, 1026, 700. ^1H NMR ($CDCl_3$): δ 1.31 (t, 6H, CH_2CH_3, J = 7.2 Hz), 4.20 (q, 4H, CH_2CH_3, J = 7.2 Hz), 7.18–7.21 (m, 4H, ArH), 7.32–7.39 (m, 6H, ArH). ^{13}C NMR ($CDCl_3$): δ 16.9 (s, CH_3); 44.3 (s, CH_2); 127.7, 128.8, 129.3, 130.5, 131.0 (s, C_{Ar}); 172.8 (s, NCN). Anal. ($C_{19}H_{20}AuBrN_2$) C, H, N.

Bromo[1,3-diethyl-4,5-bis(4-hydroxyphenyl)imidazol-2-ylidene]gold(I) 5h. Method A: yield 45.4%. Method B: yield 28.7% of a white solid. ESI-MS m/z: 813 $[2M - 2Br-Au]^+$, 1089 $[2M - Br]^+$. IR (KBr, cm^{-1}): 3600–2500 (OH), 2968, 2926, 1607, 1507, 1379, 1272, 1104, 840. ^1H NMR (DMSO-d_6): δ 1.20 (t, 6H, CH_2CH_3, J = 7.2 Hz), 4.04 (q, 4H, CH_2CH_3, J = 7.2 Hz), 6.75 (d, 4H, ArH, J = 8.4 Hz), 7.14 (d, 4H, ArH, J = 8.4 Hz), 9.78 (s, 2H, ArOH, exchangeable by D_2O). Anal. ($C_{19}H_{20}AuBrN_2O_2$) C, H, N.

Bromo[3-benzyl-1-ethyl-4,5-bis(4-methoxyphenyl)imidazol-2-ylidene]gold(I) 5i. Method A: yield 71.3% of a white solid. ESI-MS m/z: 697 $[M + Na]^+$, 993 $[2M - AuBr_2]^+$, 1269 $[2M - Br]^+$. IR (KBr, cm^{-1}): 3062, 3034, 2954, 2921, 2851, 1606, 1503, 1459, 1250, 1025, 835. ^1H NMR ($CDCl_3$): δ 1.32 (t, 3H, CH_2CH_3, J = 7.2 Hz), 3.77 (s, 3H, OCH_3), 3.78 (s, 3H, OCH_3), 4.21 (q, 2H, CH_2CH_3, J = 7.2 Hz), 5.35 (s, 2H, CH_2Ar), 6.75 (d, 2H, ArH, J = 8.8 Hz), 6.87 (q, 4H, ArH, J = 8.8 Hz), 7.02–7.10 (m, 4H, ArH), 7.21–7.23 (m, 3H, ArH). ^{13}C NMR ($CDCl_3$): δ 16.9 (s, CH_3); 44.2 (s, CH_2); 52.7 (s, CH_2Ar); 55.2 (s, OCH_3); 114.0, 114.3, 119.7, 127.5, 128.0, 128.5, 131.2, 131.3, 131.7, 132.1, 135.9 (s, C_{Ar}); 160.1 (d, C_{Ar}); 173.3 (s, NCN). Anal. ($C_{26}H_{26}AuBrN_2O_2$) C, H, N.

Bromo[3-benzyl-1-ethyl-4,5-bis(4-fluorophenyl)imidazol-2-ylidene]gold(I) 5j. Method A: yield 76.5% of a white solid. ESI-MS m/z: 673 $[M + Na]^+$, 945 $[2M - AuBr_2]^+$, 1221 $[2M - Br]^+$. IR (KBr, cm^{-1}): 3063, 3034, 2955, 2922, 2852, 1632, 1602, 1501, 1457, 1228, 1159, 829. ^1H NMR ($CDCl_3$): δ 1.35 (t, 3H, CH_2CH_3, J = 7.2 Hz), 4.23 (q, 2H, CH_2CH_3, J = 7.2 Hz), 5.37 (s, 2H, CH_2Ar), 6.92–7.08 (m, 8H, ArH), 7.16–7.24 (m, 5H, ArH). ^{13}C NMR ($CDCl_3$): δ 16.9 (s, CH_3); 44.4 (s, CH_2); 53.0 (s, CH_2Ar); 115.8, 116.0, 116.1, 116.4, 123.3, 123.4, 127.4, 128.3, 128.6, 130.7, 130.9, 132.3, 132.4, 132.7, 132.8, 135.4 (s, C_{Ar}); 161.9 (d, C_{Ar}); 164.4 (d, C_{Ar}); 174.1 (s, NCN). Anal. ($C_{24}H_{20}AuBrF_2N_2$) C, H, N.

Bromo(1,3-diethylimidazol-2-ylidene)gold(I) 5k. Method A: yield 64.3% of a white solid. ESI-MS m/z: 422 $[M + Na]^+$, 721 $[2M - Br]^+$, 824 $[2M + Na]^+$. IR (KBr, cm^{-1}): 3153, 3120, 2955, 2919, 2851, 1629, 1463, 1421, 1377, 1204, 1096, 754. ^1H NMR ($CDCl_3$): δ 1.47 (t, 6H, CH_2CH_3, J = 7.2 Hz), 4.23 (q, 4H, CH_2CH_3, J = 7.2 Hz), 6.95 (s, 2H, CH). Anal. ($C_7H_{12}AuBrN_2$) C, H, N.

General Procedure for the Synthesis of 6c and 6f. To a solution of **5c** or **5f** (0.1 mmol) in CH_2Cl_2 (2 mL) was added bromine (23.7 mg, 0.15 mmol). The mixture was stirred for 3 h in the dark, and the solvent was removed under reduced pressure, as well as the excess of bromine. The residue was recrystallized from CH_2Cl_2/n-hexane to yield **6c** or **6f** as orange powder.

Tribromo[1,3-diethyl-4,5-bis(4-methoxyphenyl)imidazol-2-ylidene]gold(III) 6c. Yield 83.1% of an orange powder. ESI-MS m/z: 795 $[M + Na]^+$. IR (KBr, cm^{-1}): 3060, 3039, 2979, 2934, 2836, 1606, 1504, 1472, 1436, 1253, 1178, 1023, 843. ^1H NMR (DMSO-d_6): δ 1.25 (t, 6H, CH_2CH_3, J = 7.2 Hz), 3.76 (s, 6H, OCH_3), 4.17 (q, 4H, CH_2CH_3, J = 7.2 Hz), 6.98 (d, 4H, ArH, J = 8.4 Hz), 7.36 (d, 4H, ArH, J = 8.8 Hz). ^{13}C NMR ($CDCl_3$): δ 15.3 (s, CH_3); 44.1 (s, CH_2); 55.3 (s, OCH_3); 114.5, 118.2, 132.0, 133.8 (s, C_{Ar}); 137.3 (s, NCN); 160.7 (s, C_{Ar}). Anal. ($C_{21}H_{24}AuBr_3N_2O_2$) C, H, N.

Tribromo[1,3-diethyl-4,5-bis(4-fluorophenyl)imidazol-2-ylidene]gold(III) 6f. Yield 85.6% of an orange powder. ESI-MS m/z: 771 $[M + Na]^+$. IR (KBr, cm^{-1}): 3110, 3062, 2984, 2936, 2875, 1629, 1600, 1503, 1474, 1343, 1228, 1159, 848. ^1H NMR ($CDCl_3$): δ 1.36 (t, 6H, CH_2CH_3, J = 7.2 Hz), 4.26 (q, 4H, CH_2CH_3, J = 7.2 Hz), 7.11 (t, 4H, ArH, J = 8.4 Hz), 7.23–7.26 (m, 4H, ArH). ^{13}C NMR ($CDCl_3$): δ 15.3 (s, CH_3); 44.3 (s, CH_2); 116.5, 116.7 (s, C_{Ar}); 121.9 (d, C_{Ar}); 132.6, 132.7, 133.2 (s, C_{Ar}); 139.4 (s, NCN); 162.3, 164.9 (s, C_{Ar}). Anal. ($C_{19}H_{18}AuBr_3F_2N_2 \cdot 0.15CH_2Cl_2$) C, H, N.

X-ray Crystallography. The intensities for the X-ray determinations were collected on a STOE IPDS 2T instrument with Mo Kα radiation (λ = 0.710 73 Å) at 200 K. Standard procedures were applied for data reduction and absorption correction. Structure solution and refinement were performed with SHELXS97 and SHELXL97.[58] Hydrogen atom positions were calculated for idealized positions and treated with the "riding model" option of SHELXL. More details on data collections and structure calculations are contained in Table 1 and Supporting Information.

Cytotoxicity. The human MCF-7, MDA-MB 231 breast cancer cell, and HT-29 colon cancer cell lines were obtained from the American Type Culture Collection. All cell lines were maintained as a monolayer culture in L-glutamine containing Dulbecco's modified Eagle's medium (DMEM) with 4.5 g/L glucose (PAA Laboratories, Austria), supplemented with 5% fetal bovine serum (FBS; Biochrom, Germany) in a humidified atmosphere (5% CO_2) at 37 °C.

The experiments were performed according to established procedures with some modifications.[10,11,35] In 96-well plates, an amount of 100 μL of a cell suspension in culture medium at 7500 cells/mL (MCF-7 and MDA-MB 231) or 3000 cells/mL (HT-29) was plated into each well and incubated for 3 days under culture conditions. After the addition of various concentrations of the test compounds, cells were incubated for up to the appropriate incubation time. Then the medium was removed, and the cells were fixed with glutardialdehyde solution 1% and stored under phosphate buffered saline (PBS) at 4 °C. Cell biomass was determined by a crystal violet staining, followed by extracting of the bound dye with ethanol and a photometric measurement at 590 nm. Mean values were calculated, and the effects of the compounds were expressed as % treated/control$_{corr}$ values according to the following equation:

$$\frac{T}{C_{corr}}(\%) = \frac{T - C_0}{C - T_0} \times 100$$

where C_0 is the control cell at the time of compound addition, C is control cell at the time of test end, and T is the probe/sample at the time of test end.

The IC_{50} value was determined as the concentration causing 50% inhibition of cell proliferation and calculated as the mean of at least two or three independent experiments (OriginPro 8).

TrxR Inhibition. To determine the inhibition of TrxR, an established microplate reader based assay was performed with minor modifications.[11,23] For this purpose, commercially available rat liver TrxR (from Sigma-Aldrich) was used and diluted with distilled water to achieve a concentration of 2.0 U/mL. The compounds were freshly dissolved as stock solutions in DMSO. To each, 25 μL aliquots of the enzyme solution, each 25 μL of potassium phosphate buffer, pH 7.0, containing the compounds in graded concentrations or vehicle (DMSO) without compounds (control probe), were added. The resulting solutions (final concentration of DMSO, 0.5% V/V) were incubated with moderate shaking for 75 min at 37 °C in a 96-well plate. To each well, an amount of 225 μL of reaction mixture (1000 μL of reaction mixture consisted of 500 μL of potassium phosphate buffer, pH 7.0, 80 μL of 100 mM EDTA solution, pH 7.5, 20 μL of BSA solution 0.05%, 100 μL of 20 mM NADPH solution, and 300 μL of distilled water) was added, and the reaction was started by addition of 25 μL of a 20 mM ethanolic DTNB solution. After proper mixing, the formation of TNB was monitored with a microplate reader (Perkin-Elmer Victor X4) at 405 nm in 10 s intervals for 6 min. The increase in TNB concentration over time followed a linear trend ($r^2 \geq 0.99$), and the enzymatic activities were calculated as the slopes (increase in absorbance per second) thereof. For each tested compound, the noninterference with the assay components was confirmed by a negative control experiment using an enzyme-free solution. The IC_{50} values were calculated as the concentration of compound decreasing the enzymatic activity of the untreated control by 50% and are given as the mean and error of repeated experiments.

Reaction with Glutathione. The gold complexes were prepared as stock solutions in DMSO and diluted with potassium phosphate buffer, pH 7.0, to achieve a final concentration of 500 μM (DMSO, 0.2% v/v). To 25 μL of 250 μM aqueous solutions of reduced glutathione, each 25 μL of the respective potassium phosphate buffer solution (containing the compounds or only the DMSO vehicle as control), an amount of 25 μL of 100 mM aqueous EDTA solution, pH 7.5, was added, and the resulting solutions were incubated with moderate shaking in a 96-well plate at 37 °C for 20 or 60 min. To each well, an amount of 200 μL of reaction mixture (1000 μL of reaction mixture consisted of 620 μL of potassium phosphate buffer, pH 7.0, 80 μL of 100 mM EDTA solution, pH 7.5, and 300 μL of distilled water) was added, and the reaction was started with the addition of 25 μL of a 20 mM ethanolic solution of DTNB. After proper mixing, the formation of TNB was monitored in a microplate reader (Perkin-Elmer Victor X4) at 405 nm. For each tested compound, the noninterference with the assay components was confirmed by a negative control experiment using a glutathione free solution. Results are presented as the mean of at least two independent experiments.

Sample Preparation for Cellular Uptake Studies. The cellular uptake was measured according to a previously described procedure.[10,47] In short, cells were grown until at least 70% confluency in 175 cm^2 cell culture flasks. Stock solutions of the gold complexes in DMF were freshly prepared and diluted with cell culture medium to the desired concentration (final DMF concentration, 0.1% v/v; final gold complex concentration, 10.0 μM). The cell culture medium of the cell culture flasks was replaced with 10 mL of the cell culture medium solutions containing the compounds, and the flasks were incubated at 37 °C/5% CO_2 for 6 h. The cell pellets were isolated by trypsinization and centrifugation (room temperature, 2000 rpm, 5 min), resuspended in twice distilled water, lysed by using a sonotrode, and appropriately diluted using twice distilled water. An aliquot was removed for the purpose of protein quantification by the Bradford method. The determination of the gold content of the samples was performed by ETAAS. Results were calculated from the data of three independent experiments and are given as ng of gold per mg of cellular protein.

Sample Preparation for Nuclear Uptake Studies. The nuclei of the tumor cells were isolated according to previously described procedures[10] with some minor modifications. Cells were grown in 175 cm^2 cell culture flasks until at least 70% confluency. The medium was removed and replaced with 10 mL of medium containing 10.0 μM drug. After 24 h of incubation at 37 °C in a humidified atmosphere, the drug containing medium was removed, cells were trypsinized, resuspended in 10 mL of cell culture medium, and isolated by centrifugation (1500 rpm, 5 min), and 0.5−1.0 mL of 0.9% NaCl solution was added. After centrifugation (1500 rpm, 5 min) pellets were resuspended in 300 μL of RSB-1 (0.01 M Tris-HCl, 0.01 M NaCl, 1.5 mM $MgCl_2$, pH 7.4) and left for 10 min in an ice bath. Swollen cells were centrifuged (2000 rpm, 5 min), resuspended in 300 μL of RSB-2 (RSB-1 containing each 0.3% v/v Nonidet-P40 and sodium desoxycholate), and homogenized by 10−15 up/down pushes in a 1 mL syringe with needle. Aliquots of 50 μL of the homogenisate were removed for determination of the total gold content and mixed with 500 μL of water. The homogenisate was centrifuged at 2500 rpm for 5 min, and the resulting crude nuclei were taken up in 150 μL of 0.25 M sucrose containing 3 mM $CaCl_2$. The suspension was underlayed with 150 μL of 0.88 M sucrose and centrifuged 10 min at 2500 rpm. The nuclei pellets were stored at −20 °C or immediately dissolved in 500 μL of water and disrupted by use of a sonotrode. The gold content of the samples was measured by ETAAS and the protein content by the Bradford method. Results are expressed as the mean of three independent experiments as ng of gold per mg of nuclear protein.

Electrothermic Atomic Absorption Spectroscopy (ETAAS). ETAAS measurements were performed according to a previously published standard addition procedure with some minor modifications.[10,47] In short, to 100 μL aliquots of the diluted lysates increasing amounts of aqueous gold standard solutions were added. All probes were adjusted to a final volume of 200 μL using twice distilled water. For each, 20 μL of Triton X-100 (1%) and ascorbic acid (1%) were added, and the probes were measured as described below. The gold content of the lysates was accessed by the linear extrapolation method. A Vario 6 electrothermal atomic absorption spectrometer (AnalytikJena AG) was used for the gold measurements. Gold was detected at a wavelength of 242.8 nm with a bandpass of 0.8 nm. A deuterium lamp was used for background correction. Probes were injected at a volume of 25 μL into regular graphite wall tubes. Drying, atomization, and tube cleaning steps were performed as outlined in more detail in the literature.[10,47] The temperature for pyrolysis was set to 1200 °C. The mean AUC (area under curve) absorptions of duplicate injections were used throughout the study. The limit of gold detection using biological samples as described above was 1.7 μg/L.

DNA Binding Studies. Precipitation of drug DNA adducts was performed according to a described method[35] with some modifications. Salmon testes DNA (Sigma) were dissolved in phosphate-buffered saline, pH 7.4, and drugs were added as stock solutions in DMF. The final solutions contained 40.6 mM drug, 250 μg/mL salmon testes DNA, and 0.1% v/v DMF. After being vortexed, the solutions were incubated at 37 °C in a water bath for 4 h. Aliquots of 200 μL were mixed with 100 μL of 0.9 M sodium acetate and three volumes of ice cold ethanol. Samples were stored at −20 °C for 30 min. The pellets were isolated by centrifugation (5000 U/min, 10 min, 4 °C) and resuspended in 300 μL of 0.3 M sodium acetate. An amount of 900 μL of ice cold ethanol was added, and the precipitate was collected after centrifugation (5000 U/min, 10 min, 4 °C). Samples were washed twice with ice cold ethanol and were stored at −20 °C. The pellets were dissolved in 500 μL of water (twice distilled), and the DNA content was determined by absorption reading at 260 nm in a UV microplate reader (Flashscan AnalytikJena AG). Salmon testes DNA dissolved in water (twice distilled) was used for calibration purposes. Samples (200 μL) for gold determination by atomic absorption spectroscopy were stabilized by addition of 20 μL of Triton X-100 (1%). The amount of drugs bound to DNA was expressed as pmol of drug per μg of DNA. Results were calculated as the mean of at least two independent experiments, which were performed with two replicates.

Estrogen Receptor Interaction. Estrogen receptor interaction studies were performed according to previously described procedures without modifications.[28,49−51,59]

Inhibition of COX Enzymes. The inhibition of isolated ovine COX-1 and human recombinant COX-2 was determined with 10 μM of the respective compounds by ELISA ("COX inhibitor screening assay", Cayman Chemicals). Experiments were performed according to the manufacturer's instructions. Absorption was measured at 415 nm (Victor 2, Perkin-Elmer). Results were calculated as the mean of duplicate determinations.

■ ASSOCIATED CONTENT

Supporting Information

^{1}H NMR and ^{13}C NMR spectra of the selected complexes (Figure S1); antiproliferative effects of cisplatin on MCF-7, MDA-MB 231, and HT-29 cells in different times and concentrations (Figure S2); detailed synthetic procedures for **1a−g**, **2a−g**, **3a−g**, and **4a−k**; crystallographic information of **5f** and **6f**; elementary analysis results of target compounds. This material is available free of charge via the Internet at http://pubs.acs.org.

■ AUTHOR INFORMATION

Corresponding Author

*Phone: +43 512 507 5245. Fax: +43 512 507 2940. E-mail: ronald.gust@uibk.ac.at.

■ ACKNOWLEDGMENTS

This work was supported by the China Scholarship Council (CSC) and the Deutsche Forschungsgemeinschaft (DFG) within FOR 630 "Biological Function of Organometallic Compounds". We are also grateful for technical support by Heike Scheffler, Gerhard Rubner, and Maxi Wenzel (Institute of Pharmacy, Freie Universität Berlin, Germany).

■ ABBREVIATIONS USED

TrxR, thioredoxin reductase; ER, estrogen receptor; SAR, structure−activity relationship; NHC, N-heterocyclic carbene; LiHMDS, lithium bis(trimethylsilyl)azide; DTNB, dithiobisnitrobenzoic acid; TNB, 2-nitro-5-thionitrobenzoic acid; ETAAS, electrothermal atomic absorption spectroscopy; COX, cyclooxygenase; LOX, lipoxygenase

■ REFERENCES

(1) Gasser, G.; Ott, I.; Metzler-Nolte, N. Organometallic anticancer compounds. *J. Med. Chem.* **2011**, *54*, 3−25.
(2) Berners-Price, S. J. Activating platinum anticancer complexes with visible light. *Angew. Chem., Int. Ed.* **2011**, *50*, 804−805.
(3) Berners-Price, S. J.; Filipovska, A. Gold compounds as therapeutic agents for human diseases. *Metallomics* **2011**, *3*, 863−873.
(4) Ott, I. On the medicinal chemistry of gold complexes as anticancer drugs. *Coord. Chem. Rev.* **2009**, *253*, 1670−1681.
(5) Nobili, S.; Mini, E.; Landini, I.; Gabbiani, C.; Casini, A.; Messori, L. Gold compounds as anticancer agents: chemistry, cellular pharmacology, and preclinical studies. *Med. Res. Rev.* **2010**, *30*, 550−580.
(6) Barnard, P. J.; Berners-Price, S. J. Targeting the mitochondrial cell death pathway with gold compounds. *Coord. Chem. Rev.* **2007**, *251*, 1889−1902.
(7) Ronconi, L.; Aldinucci, D.; Dou, Q. P.; Fregona, D. Latest insights into the anticancer activity of gold(III)-dithiocarbamato complexes. *Anti-Cancer Agents Med. Chem* **2010**, *10*, 283−292.
(8) Berners-Price, S. J.; Filipovska, A. The design of gold-based, mitochondria-targeted chemotherapeutics. *Aus. J. Chem.* **2008**, *61*, 661−668.
(9) Bindoli, A.; Rigobello, M. P.; Scutari, G.; Gabbiani, C.; Casini, A.; Messori, L. Thioredoxin reductase: a target for gold compounds acting as potential anticancer drugs. *Coord. Chem. Rev.* **2009**, *253*, 1692−1707.
(10) Scheffler, H.; You, Y.; Ott, I. Comparative studies on the cytotoxicity, cellular and nuclear uptake of a series of chloro gold(I) phosphine complexes. *Polyhedron* **2010**, *29*, 66−69.
(11) Ott, I.; Qian, X.; Xu, Y.; Vlecken, D. H.; Marques, I. J.; Kubutat, D.; Will, J.; Sheldrick, W. S.; Jesse, P.; Prokop, A.; Bagowski, C. P. A gold(I) phosphine complex containing a naphthalimide ligand functions as a TrxR inhibiting antiproliferative agent and angiogenesis inhibitor. *J. Med. Chem.* **2009**, *52*, 763−770.
(12) Mirabelli, C. K.; Johnson, R. K.; Hill, D. T.; Faucette, L. F.; Girard, G. R.; Kuo, G. Y.; Sung, C. M.; Crooke, S. T. Correlation of the in vitro cytotoxic and in vivo antitumor activities of gold(I) coordination complexes. *J. Med. Chem.* **1986**, *29*, 218−223.
(13) Krishnamurthy, D.; Karver, M. R.; Fiorillo, E.; Orrú, V.; Stanford, S. M.; Bottini, N.; Barrios, A. M. Gold(I)-mediated inhibition of protein tyrosine phosphatases: a detailed in vitro and cellular study. *J. Med. Chem.* **2008**, *51*, 4790−4795.
(14) Hickey, J. L.; Ruhayel, R. A.; Barnard, P. J.; Baker, M. V.; Berners-Price, S. J.; Filipovska, A. Mitochondria-targeted chemotherapeutics: the rational design of gold(I) N-heterocyclic carbene complexes that are selectively toxic to cancer cells and target protein selenols in preference to thiols. *J. Am. Chem. Soc.* **2008**, *130*, 12570−12571.
(15) Barnard, P. J.; Baker, M. V.; Berners-Price, S. J.; Day, D. A. Mitochondrial permeability transition induced by dinuclear gold(I) carbene complexes: potential new antimitochondrial antitumour agents. *J. Inorg. Biochem.* **2004**, *98*, 1642−1647.
(16) Jellicoe, M. M.; Nichols, S. J.; Callus, B. A.; Baker, M. V.; Barnard, P. J.; Berners-Price, S. J.; Whelan, J.; Yeoh, G. C.; Filipovska, A. Bioenergetic differences selectively sensitize tumorigenic liver progenitor cells to a new gold(I) compound. *Carcinogenesis* **2008**, *29*, 1124−1133.
(17) Bakerm, M. V.; Barnard, P. J.; Berners-Price, S. J.; Brayshaw, S. K.; Hickey, J. L.; Skelton, B. W.; White, A. H. Cationic, linear Au(I) N-heterocyclic carbene complexes: synthesis, structure and anti-mitochondrial activity. *Dalton Trans.* **2006**, 3708−3715.
(18) Barnard, P. J.; Wedlock, L. E.; Baker, M. V.; Berners-Price, S. J.; Joyce, D. A.; Skelton, B. W.; Steer, J. H. Luminescence studies of the intracellular distribution of a dinuclear gold(I) N-heterocyclic carbene complex. *Angew. Chem., Int. Ed.* **2006**, *45*, 5966−5970.
(19) Siciliano, J. T.; Deblock, C. M.; Hindi, M. K.; Durmus, S.; Panzner, J. M.; Tessier, A. C.; Youngs, J. W. Synthesis and anticancer properties of gold(I) and silver(I) N-heterocyclic carbene complexes. *J. Organomet. Chem.* **2011**, *696*, 1066−1071.
(20) Weaver, J.; Gaillard, S.; Toye, C.; Macpherson, S.; Nolan, S. P.; Riches, A. Cytotoxicity of gold(I) N-heterocyclic carbene complexes assessed by using human tumor cell lines. *Chem.—Eur. J.* **2011**, *17*, 6620−6624.
(21) Horvath, U. E. I.; Bentivoglio, G.; Hummel, M.; Schottenberger, H.; Wurst, K.; Nell, M. J.; van Rensburg, C. E. J.; Cronje, S.; Raubenheimer, H. G. A cytotoxic bis(carbene) gold(I) complex of ferrocenyl complexes: synthesis and structural characterization. *New J. Chem.* **2008**, *32*, 533−539.
(22) Ray, S.; Mohan, R.; Singh, J. K.; Samantaray, M. K.; Shaikh, M. M.; Panda, D.; Ghosh, P. Anticancer and antimicrobial metallopharmaceutical agents based on palladium, gold, and silver N-heterocyclic carbine complexes. *J. Am. Chem. Soc.* **2007**, *129*, 15042−15053.
(23) Rubbiani, R.; Kitanovic, I.; Alborzinia, H.; Can, S.; Kitanovic, A.; Onambele, L. A.; Stefanopoulou, M.; Geldmacher, Y.; Sheldrick, W. S.; Wolber, G.; Prokop, A.; Wölfl, S.; Ott, I. Benzimidazol-2-ylidene gold(I) complexes are thioredoxin reductase inhibitors with multiple antitumor properties. *J. Med. Chem.* **2010**, *53*, 8608−8618.
(24) Teyssot, M. L.; Jarrousse, A. S.; Manin, M.; Chevry, A.; Roche, S.; Norre, F.; Beaudoin, C.; Morel, L.; Boyer, D.; Mahiou, R.; Gautier, A. Metal-NHC complexes: a survey of anti-cancer properties. *Dalton Trans.* **2009**, 6894−6902.
(25) Lemke, J.; Pinto, A.; Niehoff, P.; Vasylyeva, V.; Metzler-Nolte, N. Synthesis, structural characterisation and anti-proliferative activity

of NHC gold amino acid and peptide conjugates. *Dalton Trans.* **2009**, 7063−7070.
(26) Hindi, K. M.; Panzner, M. J.; Tessier, C. A.; Cannon, C. L.; Youngs, W. J. The medicinal applications of imidazolium carbene-metal complexes. *Chem. Rev.* **2009**, *109*, 3859−3884.
(27) Liu, W.; Bensdorf, K.; Abram, U.; Niu, B.; Mariappan, A.; Gust, R. Synthesis and biological studies of silver N-heterocyclic carbene complexes derived from 4,5-diarylimidazole. *Eur. J. Med. Chem.* **2011**, *46*, 5927−5934.
(28) Gust, R.; Keilitz, R.; Schmidt, K.; von Rauch, M. Synthesis, structural evaluation, and estrogen receptor interaction of 4,5-bis(4-hydroxyphenyl)imidazoles. *Arch. Pharm.* **2002**, *335*, 463−471.
(29) Gust, R.; Beck, W.; Jaouen, G.; Schönenberger, H. Optimization of cisplatin for the treatment of hormone-dependent tumoral diseases. Part 2: Use of non-steroidal ligands. *Coord. Chem. Rev.* **2009**, *253*, 2760−2779.
(30) Baker, M. V.; Barnard, P. J.; Berners-Price, S. J.; Brayshaw, S. K.; Hickey, J. L.; Skelton, B. W.; White, A. H. Synthesis and structural characterization of linear Au(I) N-heterocyclic carbene complexes: new analogues of the Au(I) phosphine drug auranofin. *J. Organomet. Chem.* **2005**, *690*, 5625−5635.
(31) Wang, H. M. J.; Lin, I. J. B. Facile synthesis of silver(I)-carbene complexes. Useful carbene transfer agent. *Organometallics* **1998**, *17*, 972−975.
(32) Baker, M. V.; Barnard, P. J.; Brayshaw, S. K.; Hickey, J. L.; Skelton, B. W.; White, A. H. Synthetic, structural and spectroscopic studies of (pseudo) halo(1,3-di-*tert*-butylimidazol-2-ylidine)gold complexes. *Dalton Trans.* **2005**, 37−43.
(33) de Fremont, P.; Singh, R.; Stevens, E. D.; Petersen, J. L.; Nolan, S. P. Synthesis, characterization and reactivity of N-heterocyclic carbene gold(III) complexes. *Organometallics* **2007**, *26*, 1376−1385.
(34) Raubenheimer, H. G.; Cronje, S. Carbene complexes of gold: preparation, medical application and bonding. *Chem Soc. Rev.* **2008**, *37*, 1998−2011.
(35) Schlenk, M.; Ott, I.; Gust, R. Cobalt-alkyne complexes with imidazoline ligands as estrogenic carriers: synthesis and pharmacological investigations. *J. Med. Chem.* **2008**, *51*, 7318−7322.
(36) Hille, A.; Ott, I.; Kitanovic, A.; Kitanovic, I.; Alborzinia, H.; Lederer, E.; Wölfl, S.; Metzler-Nolte, N.; Schäfer, S.; Sheldrick, W. S.; Bischof, C.; Schatzschneider, U.; Gust, R. [*N*,*N*′-Bis(salicylidene)-1,2-phenylenediamine]metal complexes with cell death promoting properties. *J. Biol. Inorg. Chem.* **2009**, *14*, 711−725.
(37) Vergara, E.; Casini, A.; Sorrentino, F.; Zava, O.; Cerrada, E.; Rigobello, M. P.; Bindoli, A.; Laguna, M.; Dyson, P. J. Anticancer therapeutics that target selenoenzymes: synthesis, characterization, in vitro cytotoxicity, and thioredoxin reductase inhibition of a series of gold(I) complexes containing hydrophilic phosphine ligands. *ChemMedChem* **2010**, *5*, 96−102.
(38) Gabbiani, C.; Mastrobuoni, G.; Sorrentino, F.; Dani, B.; Rigobello, M. P.; Bindoli, A.; Laguna, M.; Pieraccini, G.; Messori, L.; Casini, A. Thioredoxin reductase, an emerging target for anticancer metallodrugs: enzyme inhibition by cytotoxic gold(III) compounds studied with combined mass spectrometry and biochemical assays. *MedChemComm* **2011**, *2*, 50−54.
(39) Coronnello, M.; Mini, E.; Caciagli, B.; Cinellu, M. A.; Bindoli, A.; Gabbiani, C.; Messori, L. Mechanisms of cytotoxicity of selected organogold(III) compounds. *J. Med. Chem.* **2005**, *48*, 6761−6765.
(40) Casini, A.; Gabbiani, C.; Sorrentino, F.; Rigobello, M. P.; Bindoli, A.; Geldbach, T. J.; Marrone, A.; Re, N.; Hartinger, C. G.; Dyson, P. J.; Messori, L. Emerging protein targets for anticancer metallodrugs: inhibition of thioredoxin reductase and cathepsin B by antitumor ruthenium(II)-arene compounds. *J. Med. Chem.* **2008**, *51*, 6773−6781.
(41) Gunatilleke, S. S.; Barrios, A. M. Inhibition of lysosomal cysteine proteases by a series of Au(I) complexes: a detailed mechanistic investigation. *J. Med. Chem.* **2006**, *49*, 3933−3937.
(42) Karver, M. R.; Krishnamurthy, D.; Kulkarni, R. A.; Bottini, N.; Barrios, A. M. Identifying potent, selective protein tyrosine phosphatase inhibitors from a library of Au(I) complexes. *J. Med. Chem.* **2009**, *52*, 6912−6918.
(43) Casini, A.; Cinellu, M. A.; Minghetti, G.; Gabbiani, C.; Coronnello, M.; Mini, E.; Messori, L. Structural and solution chemistry, antiproliferative effects, and DNA and protein binding properties of a series of dinuclear gold(III) compounds with bipyridyl ligands. *J. Med. Chem.* **2006**, *49*, 5524−5531.
(44) Ronconi, L.; Marzano, C.; Zanello, P.; Corsini, M.; Miolo, G.; Maccà, C.; Trevisan, A.; Fregona, D. Gold(III) dithiocarbamate derivatives for the treatment of cancer: solution chemistry, DNA binding, and hemolytic properties. *J. Med. Chem.* **2006**, *49*, 1648−1657.
(45) Giovagnini, L.; Ronconi, L.; Aldinucci, D.; Lorenzon, D.; Sitran, S.; Fregona, D. Synthesis, characterization, and comparative in vitro cytotoxicity studies of platinum(II), palladium(II), and gold(III) methylsarcosinedithiocarbamate complexes. *J. Med. Chem.* **2005**, *48*, 1588−1595.
(46) Mendes, F.; Groessl., M.; Nazarov, A. A.; Tsybin, Y. O.; Sava, G.; Santos, I.; Dyson, P. J.; Casini, A. Metal-based inhibition of poly(ADP-ribose) polymerase—the guardian angel of DNA. *J. Med. Chem.* **2011**, *54*, 2196−2206.
(47) Ott, I.; Scheffler, H.; Gust, R. Comparative studies on the cytotoxicity, cellular and nuclear uptake of a series of chloro gold(I) phosphine complexes. *ChemMedChem* **2007**, *2*, 702−707.
(48) Harlos, M.; Ott, I.; Gust, R.; Alborzinia, H.; Wölfl, S.; Kromm, A.; Sheldrick, W. S. Synthesis, biological activity, and structure−activity relationships for potent cytotoxic rhodium(III) polypyridyl complexes. *J. Med. Chem.* **2008**, *51*, 3924−3933.
(49) Gust, R.; Busch, S.; Keilitz, R.; Schmidt, K.; von Rauch, M. Investigations on the influence of halide substituents on the estrogen receptor interaction of 2,4,5-tris(4-hydroxyphenyl)imidazoles. *Arch. Pharm.* **2003**, *336*, 456−465.
(50) Wiglenda, T.; Gust, R. Structure−activity relationship study to understand the estrogen receptor-dependent gene activation of aryl- and alkyl-substituted 1*H*-imidazoles. *J. Med. Chem.* **2007**, *50*, 1475−1484.
(51) Wiglenda, T.; Ott, I.; Kircher, B.; Schumacher, P.; Schuster, D.; Langer, T.; Gust, R. Synthesis and pharmacological evaluation of 1*H*-imidazoles as ligands for the estrogen receptor and cytotoxic inhibitors of the cyclooxygenase. *J. Med. Chem.* **2005**, *48*, 6516−6521.
(52) Ott, I.; Schmidt, K.; Kircher, B.; Schumacher, B.; Wiglenda, T.; Gust, R. Antitumor-active cobalt-alkyne complexes derived from acetylsalicylic acid: studies on the mode of drug action. *J. Med. Chem.* **2005**, *48*, 622−629.
(53) Ott, I.; Kircher, B.; Bagowski, C. P.; Vlecken, D. H.; Ott, E. B.; Will, J.; Bensdorf, K.; Sheldrick, W. S.; Gust, R. Modulation of the biological properties of aspirin by formation of a bioorganometallic derivative. *Angew. Chem., Int. Ed.* **2009**, *48*, 1160−1163.
(54) Rubner, G.; Bensdorf, K.; Wellner, A.; Kircher, B.; Bergemann, S.; Ott, I.; Gust, R. Synthesis and biological activities of transition metal complexes based on acetylsalicylic acid as neo-anticancer agents. *J. Med. Chem.* **2010**, *53*, 6889−6898.
(55) Liu, X. H.; Rose, D. P. Differential expression and regulation of cyclooxygenase-1 and -2 in two human breast cancer cell lines. *Cancer Res.* **1996**, *56*, 5125−5127.
(56) Pereg, D.; Lishner, M. Non-steroidal anti-inflammatory drugs for the prevention and treatment of cancer. *J. Intern. Med.* **2005**, *258*, 115−123.
(57) Agrawal, A.; Fentiman, I. S. NSAIDs and breast cancer: a possible prevention and treatment strategy. *Int. J. Clin. Pract.* **2008**, *62*, 444−449.
(58) Sheldrick, G. M. *SHELXS-97 and SHELXL-97, Programs for the Solution and Refinement of Crystal Structures*; University of Goettingen: Goettingen, Germany, 1997.
(59) Schäfer, A.; Wellner, A.; Gust, R. Synthesis and investigations on the oxidative degradation of C3/C5-alkyl-1,2,4-triarylpyrroles as ligands for the estrogen receptor. *ChemMedChem* **2011**, *6*, 794−803.